Diagn Intervent Radiol 2005; 11:166-169

Radiation dose in balloon dacryocystoplasty: a study using Rando® phantoms and thermoluminescent dosimetry

Niyazi Meriç, Ülkü Rabia Yüce, Erhan T. Ilgıt

PURPOSE
The radiation dose to the lens of the eye, skin, thyroid and brain of patients who underwent diagnostic and interventional radiological procedures of the lacrimal drainage system have been measured with thermoluminescent dosimeters (TLD-100 and TLD-700) by using an adult male and female Rando® phantom. All dose values for one second of fluoroscopic exposure and one frame of digital subtraction dacryocystography (DS-DCG) exposure have been obtained individually in the pastero-anterior (PA) and lateral (LAT) projections.

MATERIALS AND METHODS
An adult male and female Rando® phantom was used instead of the patients. The procedures were performed by using an Advantx AFM C-arm unit coupled with a DX Hiline digital image acquisition and processing system. The 6-inch mode of a triple-field image intensifier (II) was used, with a circular collimation of the same or a slightly smaller size. Two different lithium floride (LiF) thermoluminescent chips were used for absorbed dose measurements: TLD700, approximately 4.5 mm in diameter and 0.9 mm in thickness; TLD100, 3.7 mm square and 0.9 mm in thickness.

RESULTS
The average values of absorbed doses (lens of the eye, skin, thyroid and brain) measured separately with TLD100 and TLD700 dosimeters after irradiation of the male and female Rando® phantom are presented for LAT and PA projections.

CONCLUSION
This study suggests that useful information for dose determination can be obtained by use of the radiation dose to the lens of the eye, thyroid and brain received during radiological procedure of the LDS for one frame of DS-DCG and one second of fluoroscopy.

Key words: • *radiation dose* • *lacrimal duct obstruction* • *interventional radiology*

From the Department of Engineering Physics (N.M. ✉ *meric@ankara.edu.tr*, Ü.R.Y.), Ankara University Faculty of Engineering, Ankara, Turkey; and the Department of Radiology (E.T.I.), Gazi University Medical School, Ankara, Turkey.

Received 21 February 2005; revision requested 4 May 2005; revision received 19 May 2005; accepted 19 May 2005.

Diagnostic and interventional radiological procedures of the head, particularly those involving the orbits, inevitably carry a risk of radiation exposure to the lens of the eye, thyroid, and brain. Balloon dacryocystoplasty (fluoroscopically guided transluminal balloon dilatation of the lacrimal drainage system), a new minimally invasive interventional radiological procedure, is a significant alternative to the surgical treatment of obstructive epiphora (1-8). The procedure, however, has a risk of radiation exposure, since radiosensitive organs such as the eyes remain in the field of the primary X-ray beam. To properly evaluate the risk/benefit ratio of this interventional radiological treatment, accurate knowledge of the ionizing radiation dose to these organs is necessary. However, assessing the dose from fluoroscopy is difficult, primarily due to the range of many parameters (kilovoltage, milliampere, field site and size, number of exposures, and fluoroscopy time). Nevertheless, many techniques have been developed for this purpose (9-11).

In this study, eye lens, thyroid, and brain doses in diagnostic and interventional radiological procedures of the lacrimal drainage system (LDS) were measured with thermoluminescent dosimeters (TLDs) by using adult male and female Rando® phantoms. Doses were measured for the postero-anterior (PA) and lateral (LAT) projections and expressed in mGy per second of fluoroscopy time or per digital image.

Materials and methods

Phantoms irradiation

Adult male and female Rando® phantoms (Alderson Research Laboratories, Stanford, CA, USA) were used for simulation. The procedures were performed by using an Advantx AFM C-arm unit coupled with a DX Hiline digital image acquisition and processing system (GE Medical Systems, Milwaukee, WI, USA). The 6-inch (15.2 cm) mode of a triple-filed (6, 9, and 15-inch) image intensifier was used with a circular collimation of the same or slightly smaller size. Digital subtraction dacryocystography (DS-DCG) in PA and/or LAT projections were performed at a rate of 1 to 2 frames per second by using the 1024x1024 acquisition matrix; fluoroscopy was limited to positioning the phantom for each projection. The distance between the under-couch X-ray tube and the image intensifier was 65 cm for PA and 76 cm for LAT projections. The image intensifier was placed as close as possible to the phantom head. The fluoroscopy was performed in the pulse progressive mode. The system was operated at 80 kVp during fluoroscopy and at 85 kVp for digital image acquisition. Total X-ray beam filtrations were measured as 2.77 and 2.83 mm aluminium, respectively. Mean values for fluoroscopic milliampere and milliampere x second settings per frame for digital image acquisition were 2

and 20, respectively. The total number of frames and fluoroscopy time were determined by the system's timer.

Thermoluminescent dosimeters

Two different lithium fluoride (LiF) TLD chips (Harshaw Chemical Company, Solon, OH, USA) were used for absorbed dose measurements: TLD700, approximately 4.5 mm in diameter and 0.9 mm in thickness; TLD100, 3.7 x 3.7 x 0.9 mm.

TLDs were irradiated with X-rays and those with responses that deviated from the mean response by 5% or more were eliminated. Between examinations, the TLDs were annealed at 400°C for one hour. After heating, the TLDs were placed on a marble surface for cooling. TLDs were read using a Model 3500 Reader (Harshaw Chemical, Solon, OH, USA).

Each chip was calibrated individually in the same radiation beam in an ionisation chamber (Rad Check Plus, Victoreen, Cleveland, OH, USA). The calibration process involved exposing the TLDs to known radiation doses and then measuring the μC output of these TLDs. These values were graphed, and the graphs were used to interpret the exposed TLDs. Background noise was systematically evaluated and subtracted from measurements before each reading.

TLDs were then placed in small plastic packets and they were attached to the phantoms. At least two TLDs per packet were used, providing the possibility to verify and compare measured values and as a contingency for the possibility that some of the TLDs were damaged.

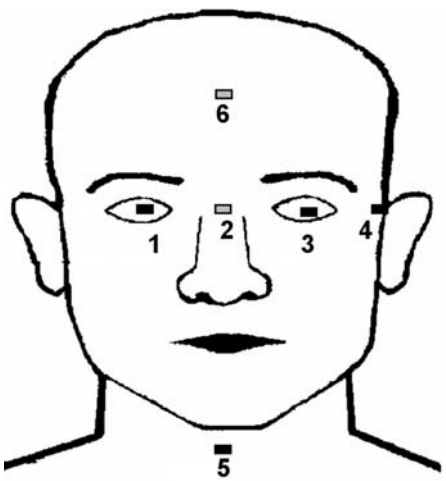

Figure. Location of TLDs. 1. Superior margin of the orbita on the right ocular bulb. 2. Occipital bone. 3. The inferior margin of the orbita on the left ocular bulb. 4. Lateral margins of the orbita. 5. Thyroid. 6. Brain.

Whenever possible, the mean value of the radiation doses measured by each set of dosimeters was calculated. As shown in Figure, doses on the eye lens were measured with the TLDs that were put on the phantom's eyes. TLDs were also placed at some given points on the occipital bone and on the lateral margins of the orbita, for the measurements of entrance skin doses for PA and LAT projections, respectively.

To determine thyroid surface exposure dose, TLDs were placed on the skin, external to the thyroid gland. One reading was taken at a point inside the brain. In the PA projections, the primary beam was directed to the LDS under study, and for LAT projections, the investigated eye was on the image intensifier side, whereas the other eye was on the tube side.

All dose values for one minute of fluoroscopic exposure and 10 frames of DS-DCG exposure were individually measured for PA and LAT projections. These values were determined based on the study by Ilgıt et al. (12). Prediction of each patient dose was carried out using these values in the equation below (Equation 1)(1);

$$D = \left[(D_F T_F) + (D_D T_D)\right]_{LAT} + \left[(D_F T_F) + (D_D T_D)\right]_{PA}$$

where D_F and D_D are the respective organ doses for one second of fluoroscopic exposure and one frame of DS-DCG exposure (1). T_F and T_D are the fluoroscopic on-times and the total number of DS-DCG frames recorded for each patient, respectively. LAT is the lateral view and PA is the posteroanterior view (10).

Calculated values of patient doses were individually compared with the values already existing in the literature using the mean relative deviation given below (Equation 2) (9);

$$\Psi = \left\{1/n \sum_{i=1}^{n} \left((D_{TLD}/D_{Lit}) - 1\right)^2\right\}^{1/2}$$

where D_{TLD} is the patient lens dose measured directly with a TLD and D_{Lit} is the patient lens dose taken from the literature.

Results

The average values of absorbed doses measured separately with TLD100 and TLD700 dosimeters after irradiation of the male and female Rando® phantoms are presented in Table 1 for LAT and PA projections. For the eye lens dose measurements, the average readings of TLDs placed on positions 1 and 3, as shown in Figure, were on the image intensifier and X-ray tube sides, respectively. Entrance skin dose measurements were made at position 4 for LAT and position 2 for PA projections; thyroid and brain readings were obtained from positions 5 and 6 respectively (see Figure again).

The total number of frames acquired during DS-DCG, fluoroscopy times, and measured radiation doses to the lens for all ten patients in this study (12) are also shown in Table 2. We have applied Equation 1 to each patient in Table 2 and calculated the radiation doses to the lens of the treated and untreated eye, skin, thyroid, and brain. We have used D_F and D_D data in Table 1. The results have been given in the last five columns of Table 2.

The mean relative deviation given by Equation 2 was used for the comparison of phantom and patient measurements. For the male patients, these deviations for treated and untreated eyes were 34% and 21%, and for the female patients they were 11.5% and 10%, respectively.

Discussion

Irradiation of the eye can cause damage to the proliferating cells in the anterior epithelium of the lens by free radical formation and oxidative effects, as well as permeability changes. These damaged cells and their breakdown products accumulate at the posterior pole of the lens and form subcapsular opacities, which are responsible for the local alterations in the index of refraction as a characteristic of cataracts (7). The other parts of the eye are relatively less sensitive to radiation damage. The threshold for X-ray induced cataract formation as a deterministic response in humans, which occurs after some delay, seems to be 2 to 10 Gy of acute exposure to low linear energy-transfer radiation (13). It is considerably higher for fractionated radiation and chronic exposure (7, 9).

In the literature, there are reports regarding the lens radiation dose in diagnostic x-ray examinations. In a study by Ilgıt et al. (12), the radiation dose to the lens during transluminal balloon dilation of the lacrimal drainage system (balloon dacryocystoplasty) was measured in 10 patients with use of thermoluminescent dosimeters placed on the

eyelids of both eyes as close as possible to the lenses. Since the examined eyes were close to the image intensifier and the untreated eyes were next to the X-ray tube, the latter were exposed to higher radiation doses. However, no appreciably significant differences were found between the absorbed dose values of the two eyes in the PA projection.

In our study, the mean relative deviations were slightly higher than those reported by Ilgıt et al. (12). This difference is attributed to statistical fluctuations. Moreover, another factor, which may account for discrepancies between the results of our Rando® phantom measurements and Ilgıt et al.'s patients' TLD measurements, may be that Rando® phantom heads are smaller than those of standard phantoms.

Although the dose for the extremity studies was directly measured with the TLD method, this study suggests that useful information for dose determination can be obtained by use of a simple factor such as D. D should be determined with a sensitive method for each X-ray beam quality and anatomical projection used in patient studies. Rando® phantom measurements can be used for this purpose and subsequent patient dose assessments can be attained using the data on fluoroscopy time and number of DS-DCG frames.

This study suggests that useful information for dose determination can be obtained by measurement of the radiation dose to the lens of the eye, thyroid, and brain, which is received during radiological procedures of the LDS, for one frame of DS-DCG and one second of fluoroscopy. Equation 1 and Table 1

Table 1. Mean dose values for one frame of digital subtraction dacryocystography and one second of fluoroscopy (mGy)

Phantom				Entrance skin dose	Untreated eye dose	Treated eye dose	Thyroid dose	Brain dose
Male	LAT	mGy/s	Fluoro (D_F)	0.223	0.198	0.033	0.004	0.032
		mGy/frame	Digital (D_D)	0.640	0.518	0.075	0.009	0.080
	PA	mGy/s	Fluoro (D_F)	0.077	0.001	0.001	0.005	0.028
		mGy/frame	Digital (D_D)	3.912	0.050	0.050	0.036	0.948
Female	LAT	mGy/s	Fluoro (D_F)	0.140	0.125	0.014	0.004	0.036
		mGy/frame	Digital (D_D)	0.404	0.330	0.033	0.008	0.090
	PA	mGy/s	Fluoro (D_F)	0.058	0.001	0.001	0.001	0.014
		mGy/frame	Digital (D_D)	3.765	0.078	0.058	0.038	0.850

LAT: lateral projection, PA: postero-anterior projection

Table 2. The comparison of Rando® phantom measurements with the related experimental data derived from reference 13, together with obtained skin, thyroid, and brain doses

	Fluoroscopy time (sec)		Number of digital images acquired		Lens dose (mGy)		Rando® phantom measurements (mGy)				
Patients (No.)	PA (T_F)	LAT (T_F)	PA (T_D)	LAT (T_D)	Treated Eye	Untreated Eye	Treated Eye*	Untreated Eye*	Skin*	Thyroid*	Brain*
Male patients											
1	1	120	24	26	5.1	39.0	7.1	38.4	137.3	1.6	28.7
2	1	210	28	0	6.1	50.4	8.2	42.9	156.3	1.9	33.3
3	264	96	12	11	4.6	24.5	4.8	25.5	95.7	2.2	22.7
4	1	258	26	12	9.1	67.8	10.6	58.5	166.9	2.1	33.9
5	1	246	31	0	6.8	60.1	9.5	50.1	176.1	2.1	37.3
6	1	12	11	10	2.8	14.7	1.7	8.1	52.2	0.5	11.6
7	1	180	9	0	4.3	30.9	6.3	36.0	75.3	1.0	14.3
Female patients											
8	108	270	9	47	2.1	47.1	5.9	50.1	96.9	1.9	23.1
9	204	228	35	0	3.2	29.8	5.4	31.4	175.4	2.4	40.8
10	126	36	18	34	1.9	20.5	2.8	17.2	93.8	1.2	21.4

*Values were obtained with Equation 1 and Table 1.

can be used for this purpose and subsequent patient dose assessments can be attained using the data on fluoroscopy time and number of DS-DCG frames. Recording these patient data also allows for retrospective dose assessment. Application of this technique to other angiographic studies will be limited when the tube output changes along with the thickness and composition of the body part under investigation during a specific examination. The addition of more projections also increases the complexity of the technique.

References

1. Song HY, Ahn HS, Park CK, Kwon SH, Kim CS, Choi KC. Complete obstruction of the nasolacrimal system I. Treatment with balloon dilation, Part I. Radiology 1993; 186:367-371.
2. Lee JM, Song HY, Han YM, et al. Balloon dacryocystoplasty: results in the treatment of complete and partial obstructions of the nasolacrimal system. Radiology 1994; 192:503-508.
3. Ilgit E, Yuksel D, Unal M, Akpek S, Isik S, Hasanreisoglu B. Transluminal balloon dilatation of the lacrimal drainage system for the treatment of epiphora. AJR Am J Roentgenol 1995; 165:1517-1524.
4. Berkefeld J, Kirchner J, Muller HM, Fries U, Kollath J. Balloon dacryocystoplasty: indications and contraindications. Radiology 1997; 205:785-790.
5. Janssen AG, Mansour K, Bos JJ. Obstructed nasolacrimal duct system in epiphora: long-term results of dacryocystoplasty by means of balloon dilation. Radiology 1997; 205:791-796.
6. Ilgit E, Yuksel D, Unal M, Akpek S, Isik S. Treatment of recurrent nasolacrimal duct obstructions with balloon-expandable metallic stents: results of early experience. AJNR Am J Neuroradiol 1996; 17:657-663.
7. Lipman RM, Tripathi BJ, Tripathi RC. Cataracts induced by microwave and ionizing radiation. Surv Ophthalmol 1988; 33:200-210.
8. Cagnon CH, Benedict SH, Mankovich NJ, Bushberg JT, Seibert JA, and Whiting JS. Exposure rates in high-level-control fluoroscopy for image enhancement. Radiology 1991; 178: 643-646.
9. Meric N, Bor D, Ilgit ET, Oznur O, Buget N. Comparison of eye lens dose measurement techniques in imaging and interventions of the lacrimal drainage system. Phys Med 1998; 14:95-100.
10. Meric N. Calculation of radiation dose to the lens of the eye using Monte Carlo Simulation. Appl Radiat Isotopes 2001; 55:557-560.
11. Meric N, Bor D, Büget N, Özkırlı M. The use of Monte Carlo technique for the determination of tissue-air ratios (TAR) in diagnostic range. Phys Medica 1998; 14:3-8.
12. Ilgıt E, Meriç N, Bor D, Öznur I, Konuş Ö, Işık S. Lens of the eye: radiation dose in balloon dacryocystoplasty. Radiology 2000; 217:54-57.
13. International Commission on Radiological Protection. 1990 Recommendations of the International Commission on Radiological Protection. Publication No. 60. In: Annals of the ICRP 21. Oxford, England: Pergamon Press, 1991.